Spheroid culture enhances osteogenic potential of periodontal ligament mesenchymal stem cells

Yuki Moritani[1], Michihiko Usui[1], Kotaro Sano[1], Kohji Nakazawa[2], Tomoya Hanatani[1], Mitsushiro Nakatomi[3], Takanori Iwata[4], Tsuyoshi Sato[5], Wataru Ariyoshi[6], Tatsuji Nishihara[6], Keisuke Nakashima[1]

[1]Division of Periodontology, Department of Oral Function, Kyushu Dental University, 2-6-1 Manazuru, Kokurakita-ku, Kitakyushu 803-8580, Japan
[2]Department of Life and Environment Engineering, The University of Kitakyushu, 1-1 Hibikino, Wakamatsu-ku, Kitakyushu 808-0135, Japan
[3]Division of Anatomy, Department of Health Promotion, Kyushu Dental University, 2-6-1 Manazuru, Kokurakita-ku, Kitakyushu 803-8580, Japan
[4]Institute of Advanced Biomedical Engineering and Science, Tokyo Women's Medical University (TWIns), 8-1 Kawada-cho, Shinjuku-ku, Tokyo 162-8666, Japan
[5]Department of Oral and Maxillofacial Surgery, Saitama Medical University, 38 Moro-hongou, Moroyama-machi, Iruma-gun, Saitama 350-0495, Japan
[6]Division of Infections and Molecular Biology, Department of Health Promotion, Kyushu Dental University, 2-6-1 Manazuru, Kokurakita-ku, Kitakyushu 803-8580, Japan

Corresponding author:

Michihiko Usui D.D.S., Ph.D
Division of Periodontology, Department of Oral Function, Kyushu Dental University, 2-6-1 Manazuru, Kokurakita-ku, Kitakyushu 803-8580, Japan
Tel: +81-93-582-1131 Fax: +81-93-582-1003 E-mail: [redacted]

Key words:

spheroid, periodontal ligament mesenchymal stem cells, osteogenesis, bone regeneration

Abstract

Objective and Background: Human periodontal ligament mesenchymal stem cells (hPDLMSC) are reported to be responsible for homeostasis and regeneration of periodontal tissue. Although hPDLMSC are commonly cultured in monolayers, monolayer cultures have been reported as inferior to three-dimensional cultures such as spheroids, which are spherical clusters of cells formed by self-assembly. The aim of this study was to examine the osteogenic phenotype of spheroids of hPDLMSC, compared with monolayer cultures of hPDLMSC, *in vitro* and *in vivo*.

Materials and Methods: Spheroids were formed using microwell chips that were tagged with polyethylene glycol (PEG). Mesenchymal stem cell (MSC) markers in hPDLMSC spheroids were examined by flow cytometer. Real-time polymerase chain reaction (PCR) analysis was examined to measure the expressions of stemness markers and osteogenesis related genes in monolayer and spheroid-cultured hPDLSMSCs. Immunofluorescence analysis was performed to confirm protein expressions of stemness markers in PDLMSC spheroid. Nodule formation assay, alkaline phosphatase (ALP) activity assay and transplantation assay in a mouse calvarial defect model were performed to confirm the osteogenic potential of hPDLMSC spheroid. To elucidate the mechanism of spheroid culture enhanced osteogenesis in hPDLMSC with osteoinductive medium (OIM), a small interfering RNA (siRNA) assay targeted with secreted frizzled-related

protein 3 (SFRP3) was examined. The levels of SFRP3 expression in monolayer and spheroid-cultured hPDLMSC with OIM were measured by real time PCR and western blotting analysis. ALP gene expression and ALP activity were examined in SFRP3 deficient hPDLMSC spheroids.

Results: The hPDLMSC spheroids expressed MSC markers, which were similar to hPDLMSC grown in monolayer cultures. Intriguingly, the protein and mRNA expressions of transcription factors that regulate 'stemness' were significantly increased in hPDLMSC spheroids, compared with hPDLMSC in monolayer cultures. Nodule formation by hPDLMSC was significantly increased in spheroid cultures grown with osteoinductive medium, compared with monolayer-cultured hPDLMSC. ALP activity and expression of osteogenesis-related genes were also significantly enhanced in hPDLMSC spheroids, compared with monolayer cultures. Treatment with hPDLMSC spheroids significantly enhanced new bone formation in a murine calvarial defect model, compared with hPDLMSC in monolayer culture. Finally, to elucidate mechanisms by which spheroid culture enhances ALP activation in hPDLMSC grown with osteoinductive medium, an siRNA assay was used to manipulate expression of SFRP3, a Wnt signaling antagonist. Knockdown of SFRP3 suppressed ALP gene expression in hPDLMSC grown in osteoinductive medium; further, it suppressed ALP activity in spheroid culture. These data suggest that the enhancement of osteogenic potential in hPDLMSC spheroids is regulated

through SFRP3-mediated ALP activation.

Conclusion: Spheroid cultures of hPDLMSC may be a novel and useful tool in regenerative medicine.

1. Introduction

Periodontal ligament mesenchymal stem cells (PDLMSC) predominate in the periodontal ligament (PDL). PDLMSC can serve as multipotent stem cells, differentiating into osteoblasts, chondoroblasts and adipocytes in the appropriate induction media (1-3); they can also differentiate into osteoblasts of alveolar bone or cementoblasts of cementum within the periodontal tissue microenvironment (1, 4). Thus, PDLMSC could be useful for regenerative therapy of periodontal tissue such as alveolar bone. Prior research has shown that the implantation of hPDLMSC—grown in monolayer culture—can regenerate periodontal tissue in animal models (5-7).

Human MSC and hPDLMSC are commonly cultured as 2D monolayers. However, many studies have shown wide differences between 2D and 3D cultures (8). 3D culture provides superior cellular heterogeneity, nutrient and oxygen gradients, cell-cell interactions, matrix deposition, and gene expression profiles (9-13). Spheroids—spherical clusters of cells formed by self-assembly—are a useful model for 3D culture (14). Recently, it was reported that spheroids of rat MSC possess enhanced osteogenic potential, compared with monolayer cultures (15).

The formation of spheroid is determined by culture environment in which cell-cell adhesion is greater than cell-material adhesion. Hanging drop culture (16, 17), round-bottomed

96-well culture (16, 18) and agitation or rotational culture (19) have been known as methods for spheroid formation. Generally, formation of a lot of spheroids can be achieved by agitation or rotational culture methods. However, these methods are difficult to control the size and diameter of spheroids. In contrast, the size and diameter of spheroids can be controlled by hanging drop culture and round-bottomed 96 well culture methods, although these methods are not suited to mass production of spheroids and pose difficulties with regard to handling. Nakazawa et al. established a procedure for spheroid formation by using microwell chips to resolve these problems. Microwell chip allows effective production homogenous spheroid and the size of spheroid can be controlled by changing the microwell scale of the chip (20). Our current study utilizes microwell chips for spheroid formation that have been tagged with polyethylene glycol (PEG) to prevent attachment to cells (20, 21). Hence, spheroids cultured in our microwell chips do not require trypsin to detach from the wells.

In this study, we examined the 'stemness' of spheroid hPDLMSC isolated from human PDL (hPDL). Furthermore, we investigated the osteogenic potential of hPDLMSC spheroids, compared with monolayer cultures via *in vitro* and *in vivo* assays, to elucidate whether hPDLMSC spheroids facilitate enhanced bone regeneration.

2. Materials and Methods

2.1. Reagents

Fluorescein isothiocyanate (FITC) mouse anti-Human CD34, CD44, CD45, CD73, CD90, CD105, CD106, CD146 and mouse immunoglobulin G1 (IgG) k Isotype control were purchased from Becton Dickinson and CD29-FITC was purchased from Beckman Coulter (Fullerton, CA, USA). An anti-SFRP3 mouse monoclonal antibody was purchased from Santa Cruz Biotechnology (Santa Cruz, CA, USA). An anti-β-actin mouse monoclonal antibody was purchased from Sigma-Aldrich (St. Louis, MO, USA). An anti-mouse IgG-HRP was obtained from GE Healthcare (Little Chalfont, England). Anti-OCT4 rabbit polyclonal antibody and anti-NANOG rabbit monoclonal antibody were purchased from Cell Signaling Technology (Danvers, MA, USA). Alex Fluor 488-conjugated goat anti-rabbit IgG was obtained from Thermo Fisher Scientific (Waltham, MA, USA). Medetomidine hydrochloride (0.3 mg/kg) (Wako; Osaka, Japan), midazolam (4 mg/kg) (Dormicum®, Astellas Pharma, Tokyo, Japan) and butorphanol tartrate (5 mg/kg) (Vetorphale®, Meiji Seika Pharma, Tokyo, Japan) were used as anesthetic agents.

2.2. Cell culture

hPDLMSC were obtained as described previously (3) under approval from Kyushu Dental University Ethics Committee (Protocol #14-21). hPDLMSC were isolated from the PDL of freshly extracted wisdom teeth; teeth were obtained from patients who were treated for

impaction, after informed consent was obtained. The wisdom teeth were extracted, washed five times with Phosphate-Buffered Saline (PBS) (Thermo Fisher Scientific) containing antibiotics (100 U/mL penicillin and 100 μg/mL streptomycin; Wako). The PDL was removed from the surface of the mid-third of the tooth root and subsequently digested in a solution of 1 mg/mL collagenase Type 1 (Wako) and 1200 PU/mL dispase (Wako) in alpha minimal essential medium (α-MEM) (Thermo Fisher Scientific) for 1 h at 37°C with shaking. Single cell suspensions were obtained by passing the cells through a 70 μm strainer (Corning, Corning, NY, USA). Then, cells were plated onto 100-mm culture dishes (Iwaki, Shizuoka, Japan) and maintained in α-MEM containing 10% fetal bovine serum (FBS; Biosera, Nuaillé, France), 100 U/mL penicillin and 100 μg/mL streptomycin (Wako), in a humidified atmosphere with 5% CO_2 at 37°C. After 24 h, unattached cells were removed and new medium was added. When confluent, cells were harvested using 0.25% trypsin and 1mM ethylenediaminetetraacetic acid (EDTA; Wako), then transferred to 150-mm culture dishes. Subculture was performed every 4 days until passage 4–5. Finally, we confirmed adipogenesis of hPDLMSC by monolayer culture with adipogenic induction medium and chondrogenesis of hPDLMSC by pellet culture with chondrogenic induction medium(data not shown).

2.3. Microwell chip

Microwell chips for hPDLMSC spheroid formation were prepared as previously published (20, 21). In present study, the microwell chip with 500 μm diameters and 500 μm depths was designed. The multimicrowell structure of the chip was fabricated by a milling system (PMT corp, Fukuoka, Japan). The chip surface was coated with a layer of platinum by using an ion sputter unit (Hitachi Hig-Tech Science Systems corp, Ibaraki, Japan). The chip was immersed in 5 mM PEG in ethanol solution and then, washed with distilled water, followed by rinsing 50% ethanol for removal of the unattached PEG and sterilization. Finally, the chip was immersed in the culture medium prior to use.

2.4. Spheroid formation

Cells were cultured at a concentration of 2,000 cells per well of microwell chips placed in a 35 mm culture dish in 2ml of α-MEM containing 10% FBS. The medium was changed every 2 days. Spheroid culturing of hPDLMSC was performed in a humidified atmosphere with 5% CO_2 at 37°C. The diameter of each spheroid colony of hPDLMSC was measured under a microscope (Olympus, Tokyo, Japan) at 6, 9, 12, 24, 48, and 72 h after harvest (n=7). To assess the cell viability of hPDLMSC in spheroid culture, a live/dead assay was performed using the Live/Dead Viability/Cytotoxicity Kit (Thermo Fisher Scientific), according to the manufacturer's protocol.

2.5. Flow cytometry analysis

After 1 day of culture, spheroid and monolayer cultures of hPDLMSC were resuspended at 10^6 cells/mL in 100 μL PBS with 2% FBS, then incubated for 30 min at 4°C with FITC-coupled primary antibodies specific for human CD29, 34, 44, 45, 73, 90, 105, 106 and 146. For isotype control, FITC-coupled nonspecific mouse IgG1 was substituted for the primary antibody. Fluorescence of cells was determined via flow cytometer (COULTER Epics XL; Beckman Coulter).

2.6. Immunofluorescence staining

The hPDLMSC were cultured in Lab-TeK Chamber Slide (Thermo Fisher Scientific) for 24 h for monolayer sample. The spheroid were also cultured in microwell chip for 24 h. The cells were fixed with 4% paraformaldehyde (PFA) (Wako) at room temperature for 20 min and incubated with 0.025% TritonX-100 (Wako) at room temperature for 5 min. After wash with PBS, the cells were blocked by 1% bovine serum albumin (BSA) (Wako) and immunostained with specific antibodies for OCT4 (#2750, Cell Signaling Technology) (1:200) and NANOG (#4903, Cell Signaling Technology) (1:400) overnight at 4 °C. After another wash with PBS, the cells were incubated with secondary antibody, Alex Fluor 488-conjugated goat anti-rabbit IgG (1:400) at room temperature for 1 h. Coverslips were mounted in Vectashield (Vector laboratories, Burlingame, CA, USA) containing 4,6-Diamidino-2-phenylindole (DAPI) to counterstain the nuclei. The cells were observed using a fluorescence microscope (BZ-9000;

Keyence, Osaka, Japan). OCT4 and NANOG positive area were measured using NIH image J software (NIH; Bethesda, MD, USA).

2.7. Real-time PCR

Real-time PCR was performed as described previously (22). Total cellular RNA was isolated from spheroid and monolayer cultures of hPDLMSC with an RNeasy mini kit (Qiagen, Hilden, Germany), according to the manufacturer's instructions. RNA was reverse transcribed with a High-Capacity RNA-to-cDNA™ Kit (Thermo Fisher Scientific) and amplified for 60 min at 37°C, then denatured for 5 min at 95°C. For real-time RT-PCR, PCR products were detected using FAST SYBR® Green Master Mix (Thermo Fisher Scientific), using the respective primer sequences shown in Table 1. Thermal cycling and fluorescence detection were performed using a StepOne™ real-time system (Applied Biosystems). Relative changes in gene expression were calculated using the comparative CT method. Total cDNA abundance between samples was normalized using primers specific to the *GAPDH* gene. The primers are listed in Table 1.

2.8. Osteogenesis assay

To induce mineralization, culture medium was changed to hMSC Osteogenic Differentiation Medium (Lonza, Basel, Switzerland) for the respective experimental time periods. The osteogenic differentiation medium was changed every other day. Microwell chip

1 was placed in a 35mm dish. In changing medium, we were careful not to aspirate spheroids in
2 microwechips. Cells were fixed with 4% PFA for 10 min and stained with 1% alizarin red
3 solution. To quantify mineralization, the area of alizarin red-positive colonies was imaged and
4 analyzed using ImageJ.

5 ***2.9. WST-8 assay***

6 The proliferation rates of monolayer and spheroid cultured hPDLMSC were measured
7 using a Cell Counting kit-8 (Doujindo, Kumamoto, Japan) according to manufacturer's
8 instruction. In brief, the hPDLMSC were seeded in 96 well plates at density 3,500 cells / well
9 for monolayer culture samples. The spheroids formed from 2,000 hPDLMSC were cultured in
10 microwell chips. On the respective time point, the cultures were then transferred to 96-well
11 plates. To each well was added 10 μL CCK-8 solution. The plates were incubated at 37°C for
12 90 min in a humidified atmosphere of 5% CO_2. The absorbance of supernatant was measured at
13 450nm.

14 ***2.10. ALP activity***

15 ALP activity was measured using the LabAssay™ ALPsystem (Wako), according to
16 the manufacturer's protocol. To measure ALP activity, the hPDLMSC from monolayer cultures
17 and spheroid cultures were washed with PBS and lysed with mammalian protein extraction
18 reagent, according to the manufacturer's instructions. ALP activity was measured using the

LabAssay™ ALPsystem (Wako) with *p*-nitrophenyl phosphate as the substrate. The optical density of *p*-nitrophenol was measured as the absorbance at 405nm. The protein content was measured with DC™ protein assay (Bio-Rad, Hercules, CA, USA) to normalize enzyme activity.

2.11. The murine calvarial bone defect model

Six-week-old female C57BL/6N mice (Kyudo, Saga, Japan) were anesthetized with an intraperitoneal injection of a mixture of anesthetic agents (Medetomidine hydrochloride (0.3 mg/kg) (Wako), midazolam (4 mg/kg) (Dormicum®, Astellas Pharma) and butorphanol tartrate (5 mg/kg) (Vetorphale®, Meiji Seika Pharma)). A calvarial bone defect on the right side, 3 mm in diameter, was created in the dorsal fragment of the parietal bone using a trephine bur (Helmut Zepf, Seitingen-Oberflacht, Germany). The mice were divided into 4 groups, defects were (1) left unfilled (sham operation; n=5); (2) filled with matrigel (Corning; n=5); (3) filled with monolayer-cultured hPDLMSC (3.0×10^4 cells), combined with matrigel (n=6); (4) filled with 15 hPDLMSC spheroids cultured for 3 days, combined with matrigel (n=6). After implantation, the periosteum and scalp were repositioned and sutured. After 2 weeks, all mice were sacrificed by anesthetic overdose. These protocols and procedures were approved by the Animal Care and Use Committee of Kyushu Dental University (Protocol #15-015).

2.12. Radiological examination of samples

After sacrifice, the site of implantation and adjacent tissue were excised, and radiological analysis was performed as follows. Dental radiography devices (90 kVp, 5.5 mA ; Panpas-E; YOSHIDA, Tokyo, Japan) were applied to evaluate bone density in the defect area. The developed dental films were captured as 2D images with a scanner (CanoScan 9950F; Canon, Tokyo, Japan), and the scanned images were analyzed using ImageJ. Bone density within the selected circular defect was calculated and all data were collected for statistical analysis by the same researcher.

2.13. Histological assessment

After radiological assessment, tissue specimens were fixed with 4% PFA (Wako) for 2 days and decalcified with Morse's solution for 3 days at 4°C. Samples were trimmed, dehydrated, and embedded in paraffin, then cut into 8 μm-thick sections and mounted on slides. Prepared slides were stained with hematoxylin/eosin to visualize histological changes. Sections were examined using a light microscope (BX50, Olympus). The following parameters were measured: (1) distance between the margins of the original surgical defect (defect length, DL); (2) length of the internal bone bridging formation (defect closure, DC); (3) total defect area (TA), determined by identifying the external and internal surfaces of the original calvarium at the right and left margins of the surgical defect, then connecting these surfaces with lines drawn along their respective curvatures; and (4) region stained with hematoxylin/eosin in the TA,

which was color-extracted and defined as newly formed bone area (NBA). The NBA was also calculated as a percentage of the TA. Linear measurement of the DC was calculated as a percentage of the defect length within each defect. The measurements of each parameter were analyzed using ImageJ.

2.14. Western blotting

Western blotting was performed as described previously (22). Cells were washed with cold PBS, and whole-cell lysates were prepared by addition of Cell Lysis Buffer (Cell Signaling Technology) that contained a protease inhibitor mixture (Thermo Fisher Scientific). Protein concentrations were measured using the DC™ protein assay kit (Bio-Rad). Equivalent amounts of protein were separated by sodium dodecyl sulfate polyacrylamide gel electrophoresis and transferred to a FluoroTrans® W Membrane (NIPPON Genetics, Tokyo, Japan). Non-specific binding sites were blocked by immersing the membrane in Blocking One buffer (Nacalai Tesque) for 30 min at room temperature. Membranes were subjected to overnight incubation with diluted primary antibodies (SFRP3 (SC-5114350; Santa Cruz), 1:1000; β-actin (A1978; Sigma–Aldrich), 1:10000) at 4°C. Membranes were then incubated with horseradish peroxidase-conjugated anti-mouse IgG as secondary antibodies (GE Healthcare) for 1 h at room temperature. After washing the membranes, chemiluminescence was produced using ECL reagent (GE Healthcare) and detected digitally with a ChemiDoc™ XRS Plus system

(Bio-Rad).

2.15. RNA interference

Small interfering RNAs (siRNAs) for SFRP3 (s5368) and the non-targeting control (4390843) were purchased from Applied Biosystems. Monolayer-cultured hPDLMSC (20,000 cells) and hPDLMSC spheroids (10 each) were plated on a 24-well plate and grown to semiconfluence. Each siRNA was used to transfect the hPDLMSC culture via Lipofectamine RNAiMAX reagent (Thermo Fisher Scientific). Cells were treated, or not treated, with osteoinductive supplements for 7 days. The cells were harvested for RNA and whole cell lysate preparation.

2.16. Statistical analysis

Data are presented as mean ± SD of five samples and all experiments were performed at least three times. Statistical analysis was performed with Statview (SAS Institute Japan, Tokyo, Japan) software, using Student's t-test and Bonferroni for comparison. p-values < 0.05 were considered to be statistically significant.

3. Results

3.1. hPDLMSC spheroid formation

First, we examined the generation of hPDLMSC spheroids from hPDL at a density of

1,000, 2,000 or 4,000 cells per well, using microwell chips. These microwell chips were tagged with PEG to prevent attachment to cells during spheroid formation (20, 21). Although spheroids formed from 2,000 and 4,000 hPDLMSC were circular, spheroids from 1,000 hPDLMSC were slightly irregular (Fig. 1A). Then, we examined spheroids from 2,000 hPDLMSC in this study. Culture of hPDLMSC in microwell chips (diameter: 500 μm) generated a single spheroid per well. At 6 h post-seeding, hPDLMSC spontaneously aggregated in the medium. The hPDLMSC aggregates formed compact multicellular spheroids 9 h post-seeding (Fig. 1B). We measured the diameter of spheroids of hPDLMSC during culture. The size of hPDLMSC spheroids decreased over time (Fig. 1C). Central necrosis has been occasionally observed in large spheroids (23). To assess cell viability, a live/dead viability/cytotoxicity assay was performed on hPDLMSC spheroid that had been cultured for 3 days. Red fluorescence indicated dead cells, while green fluorescence indicated presence of live cells. Although some dead cells were seen in hPDLMSC spheroids, most cells were viable (Fig. 1D).

3.2. Characterization of hPDLMSC spheroids

There are reports that hPDLMSC express MSC-related cell markers (2,3). To confirm expression of MSC markers in hPDLMSC spheroids, we performed fluorescence-associated cell sorting analysis, using CD29, 44, 73, 90, 105, 106 and 146 as MSC-positive markers, and CD34 and 45 as MSC-negative markers. As reported previously, monolayer-cultured hPDLMSC

strongly expressed CD29, 44, 73, 90, 105, 106 and 146, but did not express CD34 and 45 (Fig. 2A). Similarly, hPDLMSC spheroids expressed CD29, 44, 73, 90, 105, 106 and 146, but did not express CD34 and 45. We next examined expression of *OCT4* and *NANOG*, which are important transcription factors in the regulation of 'stemness,' and in the self-renewal of a variety of stem cells. Real-time PCR analysis indicated that the expression of both *OCT4* and *NANOG* was significantly increased in spheroid cultures of hPDLMSC, compared with monolayer cultures of hPDLMSC at each time point (Fig. 2B). Furthermore, we immunostained hPDLMSC in monolayer and spheroid culture to examine OCT4 and NANOG protein expression. OCT4 and NANOG protein was not expressed in monolayer cultured hPDLMSC, although most of the hPDLMSC in spheroid culture expressed OCT4 and NANOG (Fig. 2C, 2D). These data further support the notion that spheroid culture conditions can enhance the 'stemness' of hPDLMSC, compared with monolayer culture conditions.

3.3. Enhancement of osteogenesis in hPDLMSC spheroids

hPDLMSC have been shown to differentiate into osteogenic tissue (1-3). To examine the osteogenic potential of hPDLMSC spheroids, we cultured spheroid and monolayer cultures of hPDLMSC in osteoinductive medium (OIM) for 10 days. In osteogenic conditions, the monolayer-grown hPDLMSC formed few arizarin red-positive calcium deposits. In contrast, spheroid cultures of hPDLMSC were stained strongly with arizarin red (Fig. 3A). To further

compare the osteogenic potential of spheroid and monolayer cultures of hPDLMSC, we performed a nodule formation assay in monolayer conditions. We seeded hPDLMSC from monolayer culture at a density of 20,000 per well, and hPDLMSC from 10 spheroids, into a 24-well plate. After these cultures reached confluence, they were cultured in OIM for 14 days and then stained with alizarin red. The area of alizarin red-positive nodules from spheroid-derived hPDLMSC was significantly greater than monolayer-derived hPDLMSC (Fig. 3B, 3C). Spheroid cultured gingiva-derived MSC (GMSC) increased the percentage of G0 /G1 phase cells and enhanced multipotent differentiation capasities (24). It has been reported that stem cells reside in a reversible G0 phase, which is called 'quiescent' identified by lack of cell proliferation markers (25). The proliferation of hPDLMSC in monolayer and spheroid culture were assessed after 1, 2 and 3 days by Cell Counting kit-8. Although monolayer cultured hPDLMSC exhibited significantly higher proliferation rates than spheroid culture, hPDLMSC in spheroid culture were not increased (Fig. 3D). These data suggested that spheroid culture suppressed the proliferation of hPDLMSC and enhanced osteogenic potential of hPDLMSC than monolayer culture.

3.4. Osteogenic potential of hPDLMSC spheroids in a mouse calvarial bone defect model

To confirm the osteogenic potential of hPDLMSC spheroids *in vivo*, we performed a

transplantation assay, using spheroid and monolayer hPDLMSC cultures, in a mouse calvarial defect model. We first examined the ability of spheroid hPDLMSC to generate newly formed bone on calvariae, using X-ray examination. Treatment with spheroid hPDLMSC resulted in new bone formation in defects of murine calvaria at 14 day-post-surgery, whereas sham surgery did not (Fig. 4A, 4B). Treatment with monolayer-grown hPDLMSC induced significantly less new bone formation, compared with spheroid hPDLMSC treatment, as shown in soft X-ray pictures (Fig. 4A, 4B). To quantify the newly formed bone, calvariae treated with either spheroid or monolayer cultures of hPDLMSC were subjected to bone histomorphometric analysis. The percentage of defect closure by newly formed bone in calvariae treated with spheroid hPDLMSC was significantly greater than the percentage of closure in calvariae treated with monolayer hPDLMSC (Fig. 4C, 4D). Furthermore, spheroid hPDLMSC treatment resulted in a ratio of newly formed bone area/total defect area in the calvariae that was significantly enhanced, compared with treatment by monolayer hPDLMSC (Fig. 4C, 4E). These data suggest that spheroid hPDLMSC have a strong potential for bone regeneration.

3.5. Enhancement of osteogenesis by spheroid cultures of hPDLMSC through SFRP3-mediated ALP activation

To investigate whether osteogenic genes are induced in spheroid hPDLMSC treated with OIM, the expression of mRNA of the following osteogenic genes was measured by

real-time PCR: *Runt-related transcription factor 2* (*RUNX2*), *Type 1 collagen* (*COL1*), *ALP*, *osteocalcin* (*OCN*), *bonesialo protein* (*BSP*) and *osteopontin* (*OPN*). The expression of *Runx2*, *COL1* and *ALP* mRNA in spheroid hPDLMSC was significantly increased, compared with monolayer cultures of hPDLMSC, after 7 days of culture (Fig. 5A). Late markers of osteogenic differentiation, *OCN*, *BSP* and *OPN*, also showed enhanced mRNA expression in spheroid hPDLMSC, compared with monolayer cultures of hPDLMSC, after 10 days of culture (Fig. 5A). We examined the effect of spheroid culturing in OIM on the ALP activity of hPDLMSC. The ALP activity of hPDLMSC in spheroid culture was significantly increased, compared with hPDLMSC in monolayer culture (Fig. 5B). These data suggest that hPDLMSC spheroid culture enhances osteogenesis through the activation of ALP. Finally, to elucidate the mechanisms by which spheroid culture enhances ALP activation in hPDLMSC grown in OIM, we focused on SFRP3, a Wnt signaling antagonist. SFRP3 has been reported to regulate the osteoblastic differentiation of hPDLMSC (26). To analyze the expression of SFRP3 during osteogenesis in spheroid cultures grown in OIM, real-time PCR analysis and western blotting were performed. Growth in OIM increased gene and protein expression of SFRP3 in monolayer-grown hPDLMSC, as reported previously (26). Similarly, growth in OIM enhanced gene and protein expression of SFRP3 in spheroid hPDLMSC (Fig. 5C, 5E). Furthermore, SFRP3 expression in spheroid hPDLMSC was enhanced, compared with monolayer hPDLMSC, when both were

grown in OIM. On the other hand, OIM significantly suppressed *WNT5A* mRNA expression in monolayer and spheroid cultured hPDLMSC. The levels of *WNT5A* mRNA expression in OIM treated hPDLMSC spheroids were similar to monolayer cultured hPDLMSC with OIM (Fig. 5D). To confirm the role of SFRP3 in the enhancement of ALP gene expression and protein activation in spheroid hPDLMSC, a knockdown assay, utilizing siRNA of *SFRP3*, was performed. Transfection of siRNA targeting *SFRP3* significantly reduced both OIM-induced *ALP* gene expression and OIM-induced ALP activity in spheroid cultures (Fig. 5F, 5G). These data suggest that the enhancement of osteogenic potential in hPDLMSC spheroid is regulated through SFRP3-mediated ALP activation.

4. Discussion

We generated spheroid hPDLMSC using microwell chips and found that spheroid culture increased the expression of NANOG and OCT4, 'stemness' markers in hPDLMSC. Spheroid culture of human MSC (hMSC) also has been shown to increase OCT4, Sox2 and NANOG. In accordance with this enhancement by spheroid culture, expression levels of miRNAs that were involved in stem cell potency were changed, along with levels of histone H3 acetylation in K9 promoter regions of OCT4, Sox2 and NANOG (27). Various reports have indicated that hMSC undergo considerable changes in monolayer culture, although they

conserve basic features of hMSC, such as CD29, 44, 73, 90 and 105 expression, as well as osteogenic, chondrogenic and adipogenic differentiation (1-4). Cultures of hMSC that have accumulated numerous passages exhibit signs of aging and spontaneous differentiation, including increases in cell size and reduced capacities for multipotent differentiation and tissue repair (28, 29). The loss of MSC capabilities, as described above, is a hurdle for the therapeutic use of these cells. However, several passages of stem cells are essential for regenerative therapy because therapeutic tissue repair requires an abundance of cells. Thus, it is very important to develop techniques that allow stem cells to preserve their 'stemness' properties. Spheroid cultures that improve the capacities of MSC may be a useful method.

Recently, various regenerative therapies have been developed for periodontal tissue defects that result from periodontitis. The enamel matrix derivative (Emdogain) and platelet-derived growth factor have been known to promote periodontal regeneration (30). The phase III trials of Fibroblast growth factor-2 (FGF-2) have shown that FGF-2 is superior in its efficacy for regeneration of periodontal tissue, compared with Emdogain. However, even FGF-2 fills just 40% of bone defects and cannot fully repair periodontal defects (31). Therefore, novel therapies for periodontal regeneration are strongly desired. Numerous studies have evaluated the osteogenic and odontogenic regenerative capacity of PDLMSC both *in vivo* and *in vitro*, and have suggested their potential for periodontal regeneration in periodontitis patients (3, 32, 33).

Therapy involving sheets of hPDLMSC—cell sheet engineering—is an elegant method that harvests cells as an intact layer without the help of proteolytic enzymes (32). Similar to hPDLMSC sheets, the use of spheroid hPDLMSC cultures is also a favorable method that maintains an intact extracellular matrix and does not involve detachment from wells. In the present study, we used microwell chips for spheroid formation that allow formation of homogeneous spheroid colonies. This system for spheroid formation is very easy to manage, and is sufficiently high-throughput that it may prove beneficial for regenerative medicine as hPDLMSC cell sheets. Spheroid cultures of PDLMSC, generated using microwell chips, are currently under investigation for periodontal regeneration in murine periodontitis models. The periodontal tissue defect is created in the mesial furcation of maxillary first molar of SD rat using a dental round bur, which is filled hPDLMSC. The regenerated periodontal tissue including cementum, periodontal ligament and alveolar bone are examined after four weeks. Further studies are necessary for the clinical application of the PDLMSC spheroid system.

Here, we show that the spheroid form of PDLMSC enhances osteogenic potential by increasing expression of osteogenic genes, as well as ALP activation. Yamada et al. have shown that SFRP3 and SFRP4 are Wnt signaling antagonists with opposing activities: SFRP3 promotes, and SFRP4 suppresses, OIM-induced osteoblastic differentiation of hPDLMSC in monolayer culture (26). Consistent with this prior report, transfection with siRNA for *SFRP3* suppressed

OIM-induced ALP gene expression and activity in spheroid cultures of hPDLMSC (Fig. 5D, 5E). In contrast, ALP activity in spheroid cultures of hPDLMSC was not completely reduced to a comparable to a monolayer culture, upon treatment with siRNA targeting *SFRP3*; this suggests that other factors or signaling may be involved in osteogenesis of spheroid hPDLMSC. In our study, we did not clarify the function of SFRP4 in spheroid cultures of hPDLMSC, but have found that growth in OIM decreases *SFRP4* mRNA expression in spheroid cultures of hPDLMSC (data not shown). It is conceivable that SFRP4 may play a role in osteogenesis in spheroid cultures of hPDLMSC, similar to the role of SFRP3. WNT5A interacts with SFRP3 and the knockdown of WNT5A enhanced the ALP activity in hPDLMSC (26). Consistent with this paper, OIM also inhibited *WNT5A* mRNA expression in PDLMSC of both spheroid and monolayer culture in current study. Wnt signaling consists of canonical and non-canonical pathways. The non-canonical Wnt pathways inhibits the canonical pathways (34). Taken together, OIM-induced downregulation of WNT5A, a typical non-canonical WNT pathway ligands may antagonizes the canonical Wnt pathways, which then enhance osteogenesis in PDLMSC. However, there is no difference between *Wnt5A* mRNA expression in monolayer and spheroid culture. These finding suggests that downregulation of WNT5A in spheroid culture is compensated by other Wnt ligands.

We showed spheroid culture enhanced OCT4 and NANOG mRNA and protein expression in hPDLMSC, which are stem cell markers and OIM-induced osteogenesis in hPDLMSC compared to monolayer culture. Similar to our results, some researchers indicated spheroid culture in MSC increased stem cell markers such as NANOG and OCT4 (35, 36). Furthermore, Zhang et al. reported spheroid culture of GMSC enhanced NANOG and OCT4, and promoted adipocyte differentiation (24). Subbarayan et al. also showed that GMSC upregulated not only pluripotent marker, OCT4, NANOG and Sox2, and increased also bone formation related gene, OPN (37). Recently, Wada et al. have found that Semaphorin 3A (SEMA3A) induced stem cell markers including NANOG and OCT4 in PDL cells and SEMA3A overexpressing PDL cells exhibited enhanced osteogenic capacity (38). Taken together, SEMA3A may play a role in enhancement of stemness and osteogenesis in hPDLMSC spheroid. However, the detailed mechanisms that enhanced *in vitro* osteogenesis and *in vivo* bone formation by which hPDLMSC spheroids occur remain unclear. Future studies will address the detailed effects of hPDLMSC spheroids on environments during the induction of osteogeneis in bone defects. Furthermore, we found that spheroid culture suppressed cell proliferation and maintained stemness in hPDLMSC. The environment of MSCs, which is termed 'nichie' is crucial for maintaining stem cell function and preventing differentiation (39). The nichie presents ECM and facilitates cell-cell interaction. Such environment in niche acts to prevent

differentiation and maintain quiescence (40). Some researchers showed that MSC spheroids retained the functionality of bone marrow niche cells, maintaining expression of stem cell markers and downregulating cell cycle progression gene (41). Taken together, the 3D spheroid culture may provide MSC bone marrow or periodontal niche model. Our spheroid culture system using microwell chips may make a useful and relevant platform for pharmaceutical trial and regenerative medicine.

In this study, hPDLMSC spheroids with approximately 100 μm diameters were formed using a microwell chip with 500 μm diameters and depths. Sakai et al. reported that the size of spheroids can be controlled by changing scale of well in microwell chip (20). In other words, the microwell with longer diameter of the chip can form the larger size of spheroid. The relationship among the cell microsphere, the cell density and cell number is one of important factors on the spheroid culture. As an expected phenomenon, the cell density of large spheroid is lower than that of small spheroid. The cell death by the depletion of oxygen ant nutrient occurs in the center of large spheroid, which is called central necrosis. Glicklis et al. reported that spheroid from hepatocytes with a diameter of 200 μm occurred central necrosis (42). In current study, we examined characters and properties of spheroid formed from 2,000 hPDLMSC considering efficiency in murine transplantation experiment, because there is almost no difference about a diameter of spheroid between spheroids formed from 2,000 and 4,000

hPDLMSC (Fig. 1). It has not been remained unclear about good properties of spheroid for osteogenesis and bone regeneration, which are the cell number, cell density and a diameter of hPDLMSC spheroid. Our next study will focus on proper condition of hPDLMSC spheroid for periodontal tissue regeneration.

A major family of cell-surface adhesion molecules is the integrin family; these are essential proteins for spheroid formation. The expression of integrins is upregulated in spheroid-cultured osteoblasts, and inhibition of integrin expression disrupts formation of osteoblasts in spheroid cultures (43). Yamamoto et al. revealed that spheroid culture conditions promote osteoblastic differentiation of dental papilla cells, including MCS, by integrin signaling (12). It has been reported that $\alpha 2\beta 1$ integrin signaling to cell-secreted collagen may facilitate the development of osteoblastic phenotypes of MSC that are grown in spheroid culture (44). Taken together, Wnt and integrin signaling may provide key signals in the enhancement of osteogenesis in spheroid cultures of hPDLMSC. Further investigation is needed to clarify the mechanisms of the increase in osteoblastic phenotypes in spheroid-cultured hPDLMSC.

In conclusion, we have shown that spheroid culture enhances 'stemness' of hPDLMSC, and osteogenesis of hPDLMSC grown in OIM, compared with monolayer culture; our data indicate that this occurs through ALP activation. These data suggest that PDLMSC spheroids may serve as a novel and useful tool for bone regeneration.

Acknowledgments

This research was supported by JSPS KAKENHI Grant Numbers 15K20626 to T.H. and 16K11838 to M.U. We thank Ryan Chastain-Gross, Ph.D., from Edanz Group (www.edanzediting.com/ac) for editing a draft of this manuscript. The authors declare no potential conflicts of interest with respect to the authorship and publication.

References

1. Seo BM, Miura M, Gronthos S, Bartold PM, Batouli S, Brahim J, et al. Investigation of multipotent postnatal stem cells from human periodontal ligament. *Lancet.* 2004; 364(9429): 149-155.
2. Nagatomo K, Komaki M, Sekiya I, et al. Stem cell properties of human periodontal ligament cells. *J Periodontal Res.* 2006; 41(4): 303-310.
3. Iwata T, Yamato M, Zhang Z, et al. Validation of human periodontal ligament-derived cells as a reliable source for cytotherapeutic use. *J Clin Periodontol.* 2010; 37(12): 1088-1099.

4. Nojima N, Kobayashi M, Shionome M, Takahashi N, Suda T, Hasegawa K. Fibroblastic cells derived from bovine periodontal ligaments have the phenotypes of osteoblasts. *J Periodontal Res.* 1990; 25(3): 179-185.

5. Lang H, Schüler N, Nolden R. Attachment formation following replantation of cultured cells into periodontal defects--a study in minipigs. *J Dent Res.* 1998.; 77(2): 393-405.

6. Lekic PC, Rajshankar D, Chen H, Tenenbaum H, McCulloch CA. Transplantation of labeled periodontal ligament cells promotes regeneration of alveolar bone. *Anat Rec.* 2001; 262(2): 193-202.

7. Dogan A, Ozdemir A, Kubar A, Oygür T. Assessment of periodontal healing by seeding of fibroblast-like cells derived from regenerated periodontal ligament in artificial furcation defects in a dog: a pilot study. *Tissue Eng.* 2002; 8(2): 273-282.

8. Inanc B, Elcin AE, Elcin YM. Osteogenic induction of human periodontal ligament fibroblasts under two- and three-dimensional culture conditions. *Tissue Eng.* 2006; 12(2): 257-266.

9. Rutherford RB, Moalli M, Franceschi RT, Wang D, Gu K, Krebsbach PH. Bone morphogenetic protein-transduced human fibroblasts convert to osteoblasts and form bone in vivo. *Tissue Eng.* 2002; 8(3): 441-452.

10. Wiesmann HP, Nazer N, Klatt C, Szuwart T, Meyer U. Bone tissue engineering by primary osteoblast-like cells in a monolayer system and 3-dimensional collagen gel. *J Oral Maxillofac Surg.* 2003; 61(12): 1455-1462.

11. Cheng NC, Wang S, Young TH. The influence of spheroid formation of human adipose-derived stem cells on chitosan films on stemness and differentiation capabilities. *Biomaterials.* 2012.; 33(6): 1748-1758.

12. Yamamoto M, Kawashima N, Takashino N, et al. Three-dimensional spheroid culture promotes odonto/osteoblastic differentiation of dental pulp cells. *Arch Oral Biol.* 2014; 59(3): 310-317.

13. Yeh HY, Liu BH, Sieber M, Hsu SH. Substrate-dependent gene regulation of self-assembled human MSC spheroids on chitosan membranes. *BMC Genomics.* 2014; 15: 10.

14. Petrenko Y, Syková E, Kubinová Š. The therapeutic potential of three-dimensional multipotent mesenchymal stromal cell spheroids. *Stem Cell Res Ther.*. 2017; 8: 94.

15. Yamaguchi Y, Ohno J, Sato A, Kido H, Fukushima T. Mesenchymal stem cell spheroids exhibit enhanced in-vitro and in-vivo osteoregenerative potential. *BMC Biotechnol.* 2014; 14: 105.

16. Dang SM, Kyba M, Perlingeiro R, Daley GQ, Zandstra PW. Efficiency of embryoid body formation and hematopoietic development from embryonic stem cells in different culture systems. *Biotechnol Bioeng.* 2002; 78(4): 442-453.

17. Kelm JM, Timmins NE, Brown CJ, Fussenegger M, Nielsen LK. Method for generation of homogeneous multicellular tumor spheroids applicable to a wide variety of cell types. *Biotechnol Bioeng.* 2003; 83(2): 173-80.

18. Koike M, Sakaki S, Amano Y, Kurosawa H. Characterization of embryoid bodies of mouse embryonic stem cells formed under various culture conditions and estimation of differentiation status of such bodies. *J Biosci Bioeng.* 2007; 104(4): 294-9.

19. Fok EY, Zandstra PW. Shear-controlled single-step mouse embryonic stem cell expansion and embryoid body-based differentiation. *Stem Cells.* 2005; 23(9): 1333-42.

20. Sakai Y, Yoshida S, Yoshiura Y, et al. Effect of microwell chip structure on cell microsphere production of various animal cells. *Journal of Bioscience and Bioengineering.* 2010; 110(2): 223-229.

21. Sakai Y, Nakazawa K. Technique for the control of spheroid diameter using microfabricated chips. *Acta Biomater.* 2007; 3(6): 1033-1040.

22. Usui M, Sato T, Yamamoto G, et al. Gingival epithelial cells support osteoclastogenesis by producing receptor activator of nuclear factor kappa B ligand via protein kinase A signaling. *J Periodontal Res.* 2015; 51(4): 462-470.

23. Friedrich J, Eder W, Castaneda J, et al. A Reliable Tool to Determine Cell Viability in Complex 3-D Culture: The Acid Phosphatase Assay. *J Biomol Screen.* 2007; 12(7): 925-937.

24. Zhang Q, Nguyen AL, Shi S, Hill C, Wilder-Smith P, Krasieva TB, Le AD. Three-Dimensional Spheroid Culture of Human Gingiva-Derived Mesenchymal Stem Cells Enhances Mitigation of Chemotherapy-Induced Oral Mucositis. *Stem Cells Dev.* 2012; 21(6): 937-47.

25. Cheung TH, Rando TA. Molecular regulation of stem cell quiescence. Nat Rev *Mol Cell Biol.* 2013;14(6):329-40.

26. Yamada A, Iwata T, Yamato M, Okano T, Izumi Y. Diverse functions of secreted frizzled-related proteins in the osteoblastogenesis of human multipotent mesenchymal stromal cells. *Biomaterials.* 2013; 34(13): 3270-3278.

27. Guo L, Zhou Y, Wang S, Wu Y. Epigenetic changes of mesenchymal stem cells in three-dimensional (3D) spheroids. *J Cell Mol Med.* 2014; 18(10): 2009-2019.

28. Krampera M, Pasini A, Rigo A, et al. HB-EGF/HER-1 signaling in bone marrow mesenchymal stem cells: inducing cell expansion and reversibly preventing multilineage differentiation. *Blood.* 2005; 106(1): 59-66.

29. Li Z, Liu C, Xie Z, et al. Epigenetic dysregulation in mesenchymal stem cell aging and spontaneous differentiation. *PLoS One.* 2011; 6(6): e20526.

30. Giannobile WV, Somerman MJ. Growth and Amelogenin-Like Factors in Periodontal Wound Healing. A Systematic Review. *Ann Periodontol.* 2003; 8(1): 193-204.

31. Kitamura M, Akamatsu M, Kawanami M, et al. Randomized Placebo-Controlled and Controlled Non-Inferiority Phase III Trials Comparing Trafermin, a Recombinant Human Fibroblast Growth Factor 2, and Enamel Matrix Derivative in Periodontal Regeneration in Intrabony Defects. *J Bone Miner Res.* 2016; 31(4): 806-14.

32. Iwata T, Yamato M, Tsuchioka H, et al. Periodontal regeneration with multi-layered periodontal ligament-derived cell sheets in a canine model. *Biomaterials.* 2009; 30(14): 2716-2723.

33. Tsumanuma Y, Iwata T, Washio K, et al. Comparison of different tissue-derived stem cell sheets for periodontal regeneration in a canine 1-wall defect model. *Biomaterials.* 2011; 32(25): 5819-5825.

34. Nemeth MJ, Topol L, Anderson SM, Yang Y, Bodine DM. Wnt5a inhibits canonical Wnt signaling in hematopoietic stem cells and enhances repopulation. Proc Natl Acad Sci U S A. 2007; 104(39):15436-41.

35. Huang GS, Dai LG, Yen BL, Hsu SH. Spheroid formation of mesenchymal stem cells on chitosan and chitosan-hyaluronan membranes. *Biomaterials.* 2011; 32(29): 6929-45.

36. Cheng NC, Wang S, Young TH. The influence of spheroid formation of human adipose-derived stem cells on chitosan films on stemness and differentiation capabilities. *Biomaterials.* 2012; 33(6): 1748-58.

37. Subbarayan R, Murugan Girija D, Mukherjee J, Mamidanna SRR, Ranga Rao S. Comparision of Gingival and Umbilical Cord Stem Cells Based on Its Modulus and Neuronal Differentiation. *J Cell Biochem.* 2017; 118(8): 2000-2008.

38. Wada N, Maeda H, Hasegawa D, Gronthos S, Bartold PM, Menicanin D, Fujii S, Yoshida S, Tomokiyo A, Monnouchi S, Akamine A. Semaphorin 3A induces mesenchymal-stem-like properties in human periodontal ligament cells. *Stem Cells Dev.* 2014; 23(18): 2225-36.

39. Engler AJ, Sen S, Sweeney HL et al. Matrix elasticity directs stem cell lineage specification. Cell. 2006(4); 126: 677–689.

40. Chen X-D, Dusevich V, Feng JQ et al. Extracellular matrix made by bone marrow cells

facilitates expansion of marrow-derived mesenchymal progenitor cells and prevents their differentiation into osteoblasts. J Bone Miner Res 2007; 22(12): 1943–56.

41. Lewis NS, Lewis EE, Mullin M, Wheadon H, Dalby MJ, Berry CC. Magnetically levitated mesenchymal stem cell spheroids cultured with a collagen gel maintain phenotype and quiescence. J Tissue Eng. 2017; 8:2041731417704428.

42. Glicklis R, Merchuk JC, Cohen S. Modeling mass transfer in hepatocyte spheroids via cell viability, spheroid size, and hepatocellular functions. *Biotechnol Bioeng*. 2004; 20;86(6):672-80.

43. Hynes RO. Integrins: bidirectional, allosteric signaling machines. *Cell.* 2002; 110(6): 673-687.

44. Murphy KC, Hoch AI, Harvestine JN, Zhou D, Leach JK. Mesenchymal Stem Cell Spheroids Retain Osteogenic Phenotype Through α2β1 Signaling. *Stem Cells Transl Med.* 2016; 5(9): 1229-1237.

Figure Legends

Figure 1. Formation of hPDLMSC spheroids.

(A) Photograph of spheroid colonies from 1,000, 2,000 or 4,000 hPDLMSC during culture (1-3 days). Spheroid formed from 1,000 hPDLMSC is irregular compared with 2,000 and 4,000 hPDLMSC. Scale bar shows 100 μm. (B) Photograph of hPDLMSC spheroid colonies during culture (3–72 h). The hPDLMSC aggregated 6 h after harvest and formed spheroids in microwell chips. Scale bar shows 100 μm. (C) Change in diameter of hPDLMSC spheroids during culture. The diameter of hPDLMSC spheroids (n=7) significantly decreased after 24 h. * $p< 0.05$ (compared with 6 h). (D) Live and dead staining of hPDLMSC spheroids at 6, 9, 12, 24, 48 and 72 h. Live cells were stained green and dead cells were stained red. Few red cells were found inside hPDLMSC spheroids. Scale bar shows 100 μm.

Figure 2. Expressions of MSC markers and 'stemness' markers in hPDLMSC spheroids.

(A) Expression of MSC-positive and MSC-negative markers in monolayer and spheroid cultures of hPDLMSC for 24 h. The MSC-positive markers CD29, 44, 73, 90, 105, 106 and 146 were expressed in spheroid cultures of hPDLMSC at concentrations similar to those observed in monolayer culture. In contrast, CD34 and 45, which are hematopoietic markers, were not expressed in spheroid cultures of hPDLMSC, similar to observations of hPDLMSC grown in monolayer culture. Isotype-matched IgG was used as negative control. Red: isotype control, blue: MSC positive or negative marker. (B)

Expression of 'stemness' markers in hPDLMSC grown in monolayer and spheroid culture. The levels of both *OCT4* and *NANOG* expression in hPDLMSC spheroids were significantly higher than those observed in monolayer culture on each time point. * $p< 0.05$ (compared with monolayer culture). (C) Immunofluorescence staining of NANOG and OCT4. The hPDLMSC were cultured in monolayer and spheroid condition for 1 day. Monolayer and spheroid cultured hPDLMSC fixed in 4% PFA were immunostained with primary antibodies specific for OCT4 and NANOG. Scale bar shows 100 μm. (D) The percentage of OCT4 and NANOG antibodies positive area in hPDLMSC spheroid. The areas stained with green were measured by NIH image J.

Figure 3. Enhancement of Osteogenic differentiation in hPDLMSC from spheroid culture in vitro.

(A) Osteogenic differentiation of hPDLMSC spheroids in 3D culture. Spheroid and monolayer cultures of hPDLMSC were grown in osteoinductive medium for 10 days. Whole hPDLMSC spheroids were alizarin red positive, while hPDLMSC in monolayer cultures appeared only partially stained with alizarin red. Scale bar shows 100 μm. (B, C) Osteogenic differentiation of hPDLMSC from spheroid culture and monolayer culture. The hPDLMSC from both spheroid and monolayer cultures were incubated in monolayer conditions until confluent in normal medium. Cells were then cultured for 14 days in osteoinductive medium and stained with alizarin red (B). The area of alizarin red-positive nodules formed by hPDLMSC from spheroid

culture was comparatively greater than hPDLMSC from the monolayer culture (C). * $p< 0.05$. (D) Proliferation in spheroid cultured hPDLMSC. spheroid and monolayer culture were grown in normal medium for 1, 2 and 3 days. The proliferation rates of spheroid and monolayer cultured hPDLMSC were measured by Cell Counting kit-8. * $p< 0.05$ (compared with Day1 monolayer culture).

Figure 4. New bone formation by hPDLMSC from spheroid culture in a mouse calvaria defect model.

(A) X-ray images of parietal bone at 14 days after transplantation of matrigel, hPDLMSC from monolayer culture or hPDLMSC from spheroid culture. Matrigel was used as a scaffold for hPDLMSC. The spheroid hPDLMSC treatment formed new bone in a defect of parietal bone. (B) Calvariae bone volume after treatment with matrigel, hPDLMSC from monolayer culture or hPDLMSC from spheroid culture was quantitatively examined using an image analyzer. (C) Photographs of histological sections that were representative of the sham surgery group, the matrigel transplantation group, the monolayer-cultured hPDLMSC transplantation group and the spheroid hPDLMSC transplantation group at 14 days after operation. These sections were stained with hematoxylin/eosin. Solid lines indicate the edge of host bone. The area between the solid lines shows a defect by trephine bur, while the areas between solid and dotted lines show newly formed bone. (D, E) Bone histomorphometric analyis of new bone formation following

treatment with hPDLMSC from either spheroid or monolayer cultures. The percentage of defect closure / defect length (panel D) and the rate of new bone formation / total defect area (panel E) were calculated in each group.

Figure 5. Enhancement of osteogenesis of spheroid hPDLMSC through SFRP3-mediated ALP activation.

(A) The expression of osteogenesis-related genes in spheroid and monolayer hPDLMSC cultured with osteoinductive medium (OIM) on Days 7, 10 and 14. The expression of *RUNX2*, *COL1*, *ALP*, *OCN*, *BSP* and *OPN* mRNA were significantly increased in spheroid hPDLMSC, compared with monolayer hPDLMSC. * $p< 0.05$. (B) ALP activation within monolayer and spheroid hPDLMSC cultured with OIM on Days 0, 7, 10 and 14. ALP activation was significantly enhanced in spheroid hPDLMSC, compared with monolayer culture, on each day. * $p< 0.05$. (C, D and E) *SFRP3* and *WNT5A* mRNA expression and SFRP3 protein expression in monolayer and spheroid hPDLMSC, cultured with or without OIM. The expressions of *SFRP3* and *WNT5A* mRNA were examined on Days 3, 5, 7 and 10 by real-time RT-PCR (C, D). The expression of SFRP3 protein was examined on Day 7 by western blotting analysis (E). Culture in OIM increased gene and protein expression of SFRP3 in both monolayer and spheroid cultures of hPDLMSC. The expression of *SFRP3 mRNA* was significantly enhanced in spheroid hPDLMSC, compared with monolayer hPDLMSC. * $p< 0.05$. (F, G) Monolayer-cultured

hPDLMSC and spheroid hPDLMSC (2,000 cells/spheroid) were plated on a dish for comparative monolayer culture. The siRNA for SFRP3 or the control were transfected into the cells, which were then treated with or without OIM for 7 days. (F) Effects of siSFRP3 on *ALP* mRNA expression in monolayer and spheroid hPDLMSC cultured with OIM. On Day 7, expression of *ALP* mRNA was examined by real-time RT-PCR. * $p< 0.05$. (G) Effects of siSFRP3 on ALP activity in monolayer and spheroid hPDLMSC cultured with OIM. On Day 7, expression of ALP activity was measured. * $p< 0.05$.

1

2 Table 1. Primers Sequence for realtime RT-PCR

3

Genes	Sequences of primers
GAPDH	F: 5'-GAAGGTGAAGGTCGGAGTC-3'
	R: 3'-GAAGATGGTGATGGGATTTC-5'
OCT4	F: 5'-AGCAAAACCCGGAGGAGT-3'
	R: 3'-CCACATCGGCCTGTGTATATC-5'
NANOG	F: 5'-TGAACCTCAGCTACAAACAG-3'
	R: 3'-TGGTGGTAGGAAGAGTAAAG-5'
RUNX2	F: 5'-AACCCTTAATTTGCACTGGGTCA-3'
	R: 3'-CAAATTCCAGCAATGTTTGTGCTAC-5'
COL1	F: 5'-AGGGCTCCAACGAGATCGAGATCCG-3'
	R: 3'-TACAGGAAGCAGACAGGGCCAACGTCG-5'
ALP	F: 5'-ACGTGGCTAAGAATGTCATC-3'
	R: 3'-CTGGTAGGCGATGTCCTTA-5'
OPN	F: 5'-CCAAGTAAGTCCAACGAAAG-3'
	R: 3'-GGTGATGTCCTCGTCTGTA-5'
BSP	F: 5'-AAAACGAAGAAAGCGAAGC-3'

	R: 3'-TATTCATTGACGCCCGTGTA-5'
OCN	F: 5'-GGTGCAGCCTTTGTGTCCAA-3'
	R: 3'-CCTGAAAGCCGATGTGGTCA-5'
SFRP3	F: 5'-CTCATCAAGTACCGCCACTCGTG-3'
	R: 3'-CCGGAAATAGGTCTTCTGTGTAGCTC-5'
WNT5A	F: 5'-CAAGGGCTCCTACGAGAGTGC-3'
	R: 3'-GCCGCGCTGTCGTACTTCT-5'

1

Fig. 1

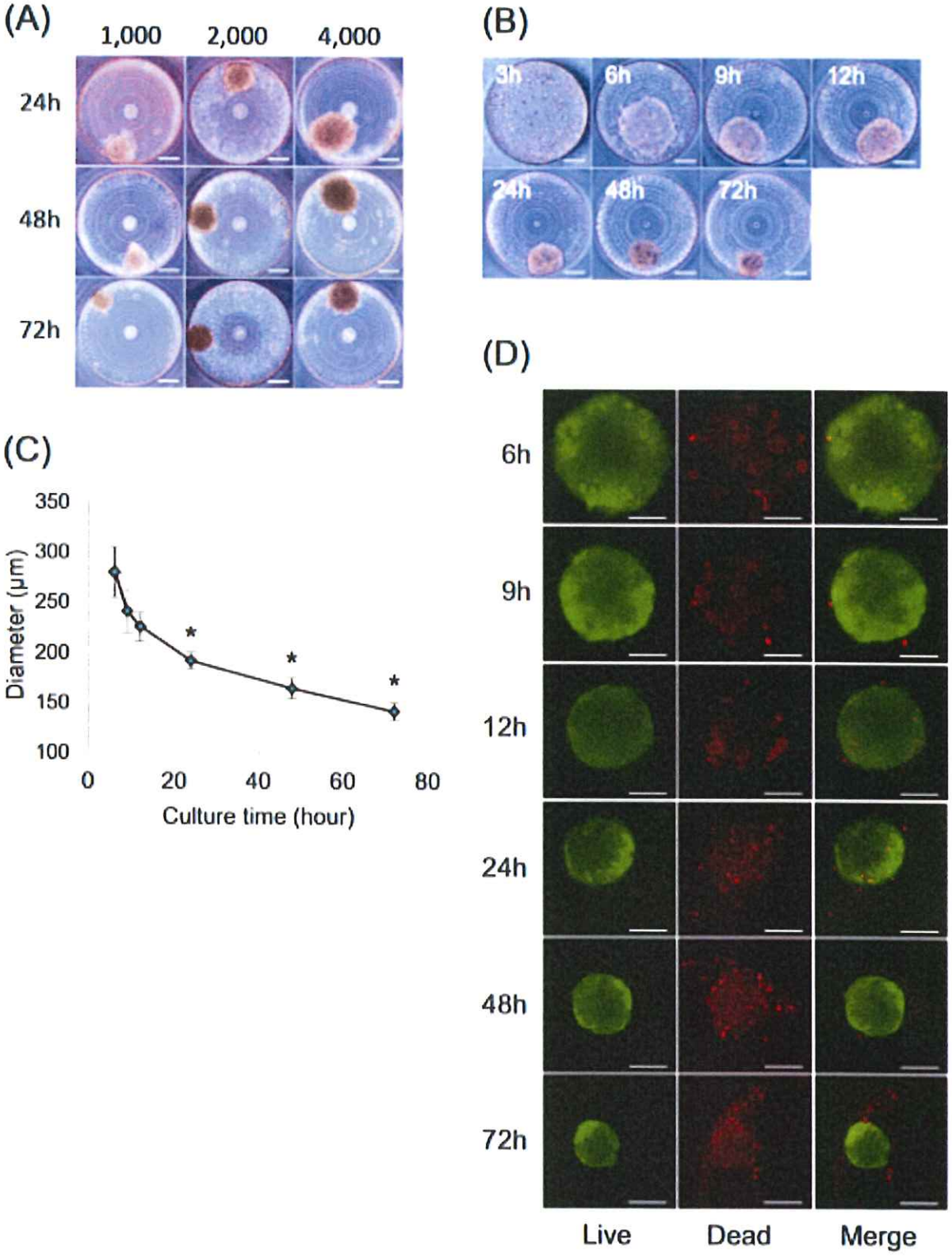
(A)
1,000
2,000
4,000
24h
48h
72h
(B)
3h
6h
9h
12h
24h
48h
72h
(C)
Diameter (μm)
350
300
250
200
150
100
0
20
40
60
80
Culture time (hour)
(D)
6h
9h
12h
24h
48h
72h
Live
Dead
Merge

Fig. 2

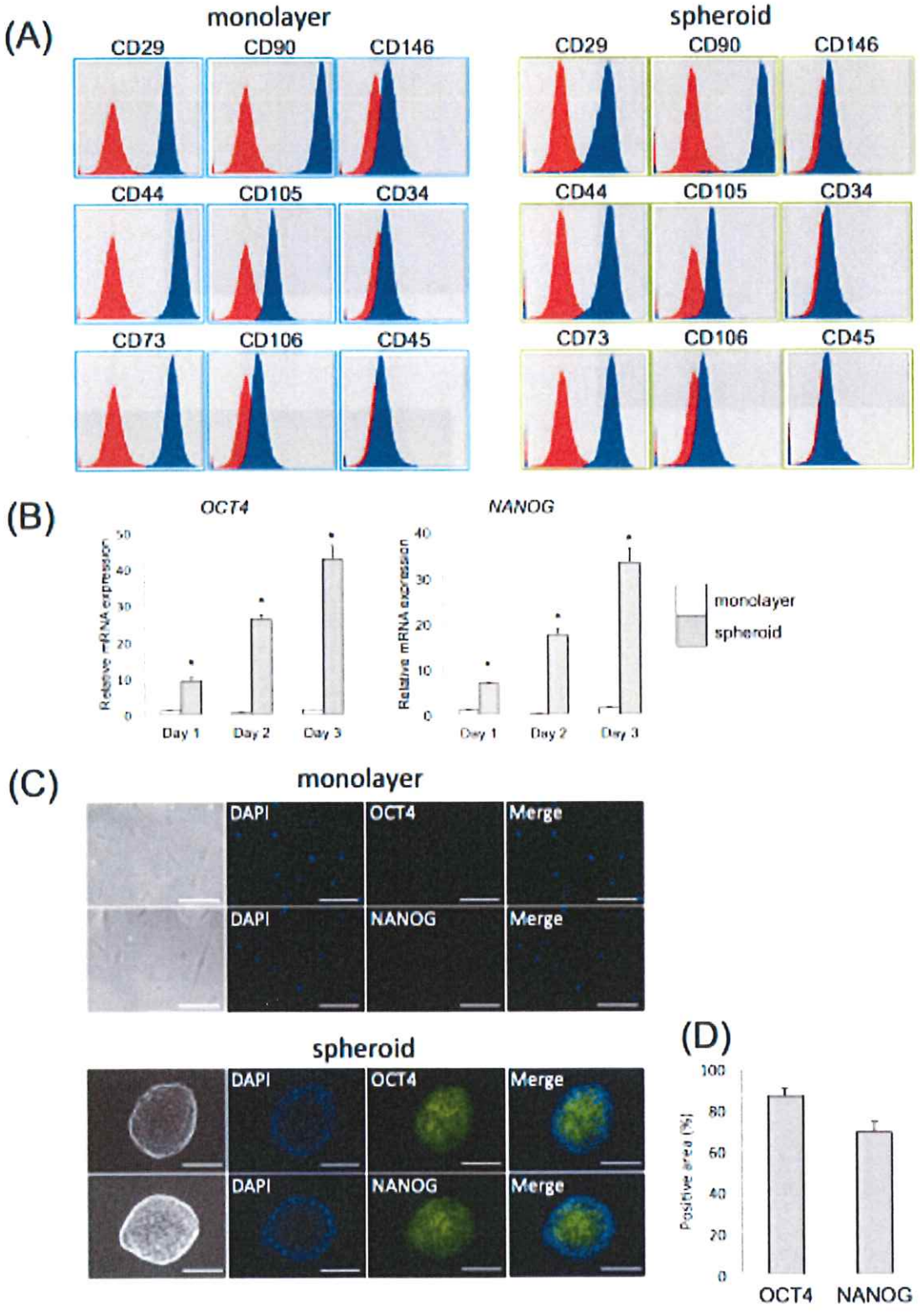
(A)
monolayer
spheroid
CD29
CD90
CD146
CD44
CD105
CD34
CD73
CD106
CD45
(B)
OCT4
NANOG
Relative mRNA expression
Day 1
Day 2
Day 3
monolayer
spheroid
(C)
monolayer
DAPI
OCT4
Merge
DAPI
NANOG
Merge
spheroid
DAPI
OCT4
Merge
DAPI
NANOG
Merge
(D)
Positive area (%)
OCT4
NANOG

Fig. 3

(A)

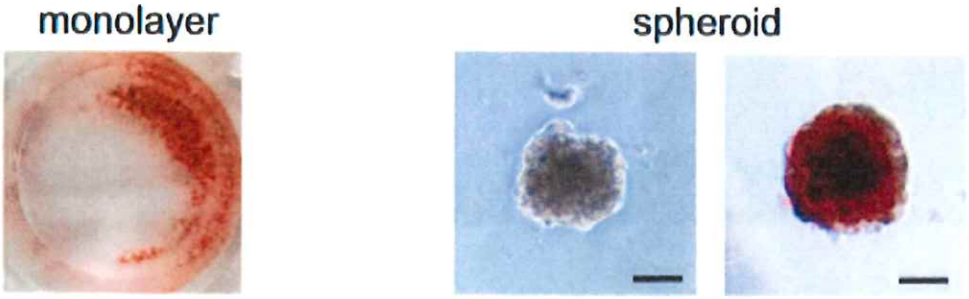
monolayer
spheroid

(B)

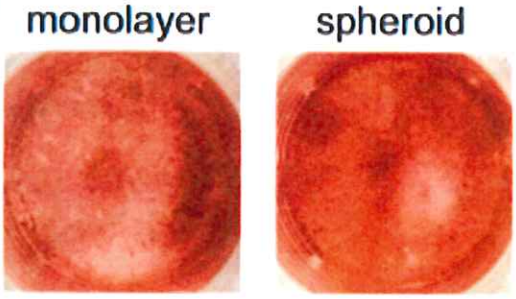
monolayer
spheroid

(C)

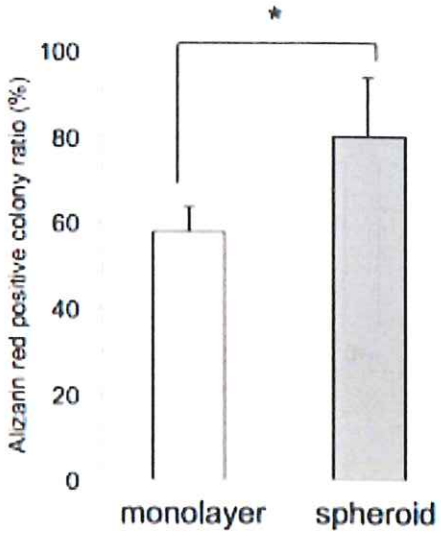
*
100
80
60
40
20
0
Alizann red positive colony ratio (%)
monolayer
spheroid

(D)

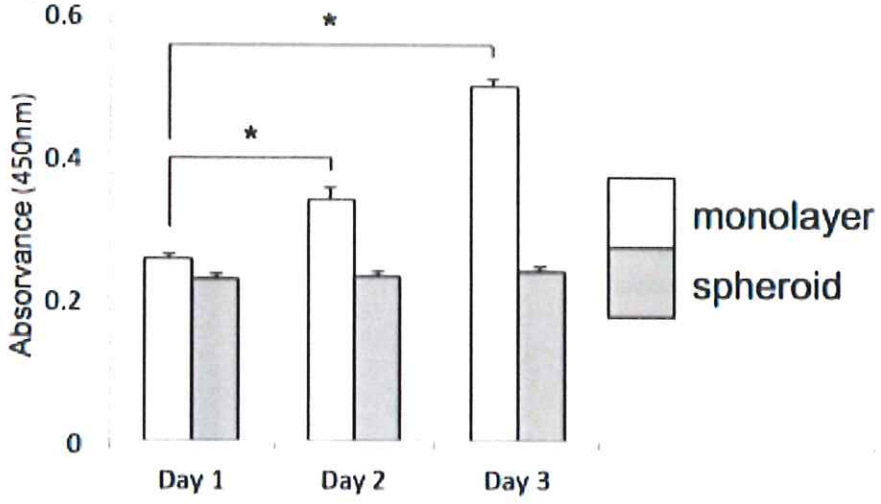
0.6
0.4
0.2
0
Absorvance (450nm)
*
*
Day 1
Day 2
Day 3
monolayer
spheroid

Fig. 4

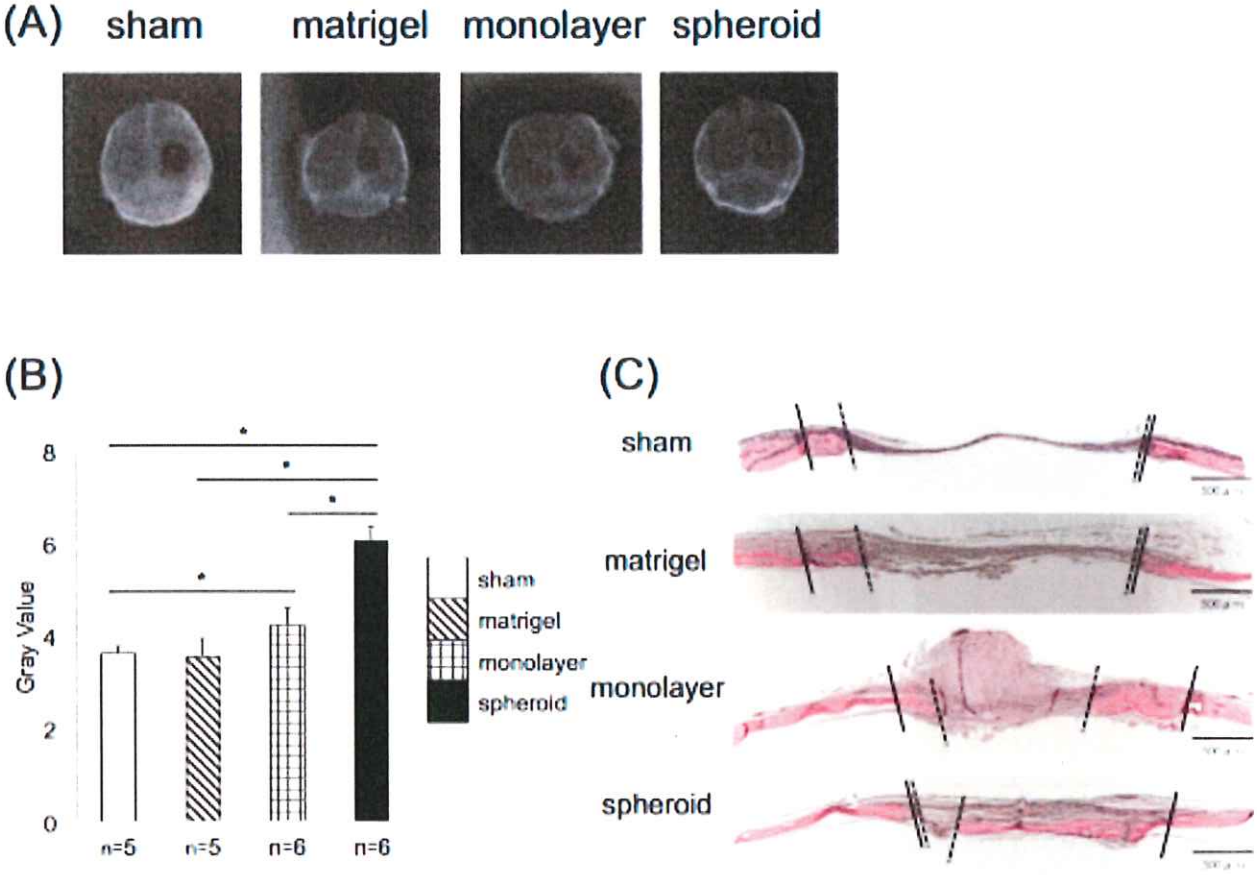
(A)
sham
matrigel
monolayer
spheroid
(B)
Gray Value
0
2
4
6
8
n=5
n=5
n=6
n=6
sham
matrigel
monolayer
spheroid
(C)
sham
matrigel
monolayer
spheroid
(D)
Defect closure / defect length
0%
20%
40%
60%
80%
100%
n=5
n=5
n=6
n=6
sham
matrigel
monolayer
spheroid
(E)
New bone formation / total defect area
0%
20%
40%
60%
80%
100%
n=5
n=5
n=6
n=6
sham
matrigel
monolayer
spheroid

Fig. 5

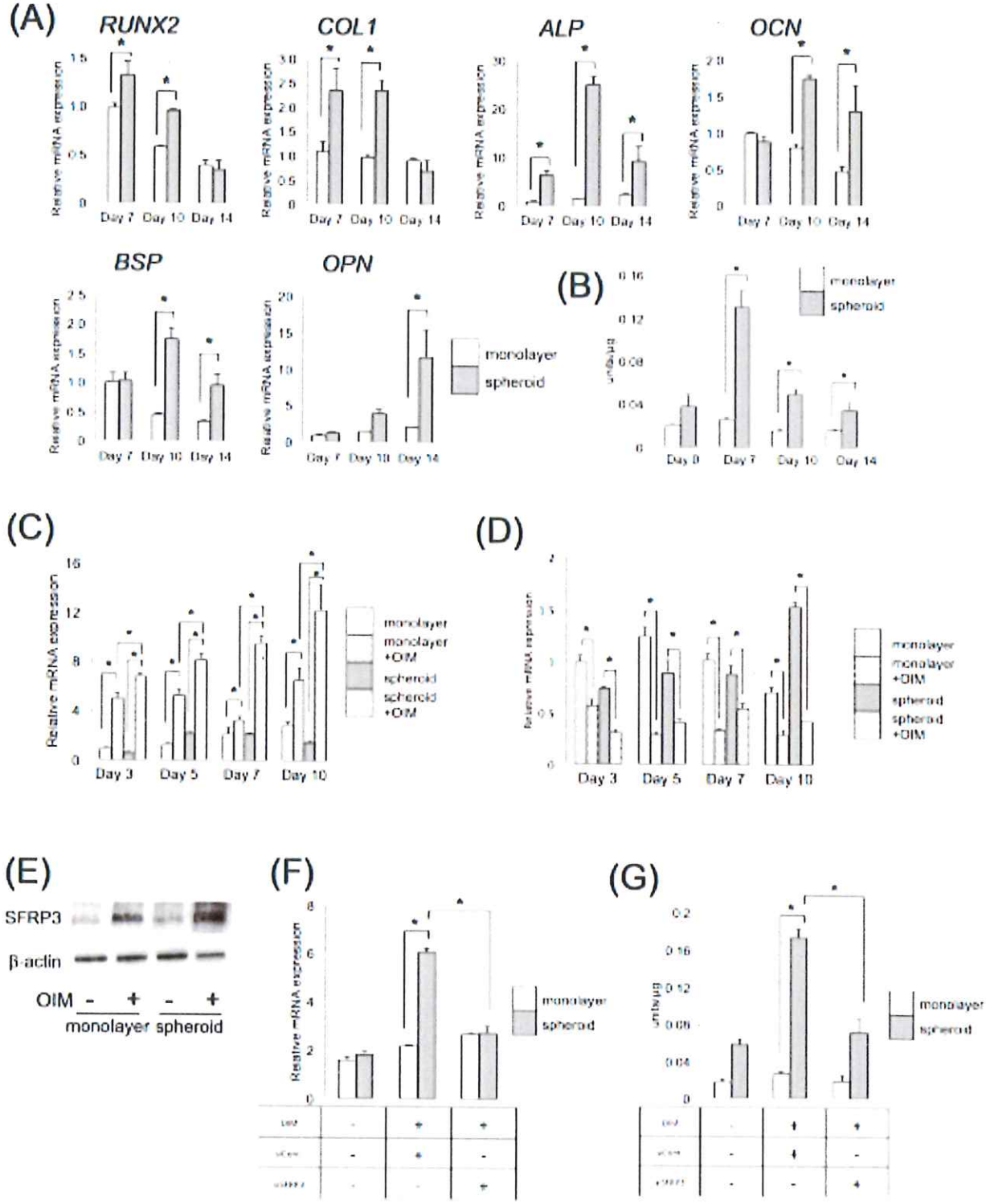
(A)
RUNX2
COL1
ALP
OCN
BSP
OPN
Relative mRNA expression
Day 7
Day 10
Day 14
monolayer
spheroid
(B)
Day 0
Day 7
Day 10
Day 14
(C)
Relative mRNA expression
Day 3
Day 5
Day 7
Day 10
monolayer
monolayer +OIM
spheroid
spheroid +OIM
(D)
(E)
SFRP3
β-actin
OIM - + - +
monolayer spheroid
(F)
(G)